# **RSC Advances**



## **PAPER**

View Article Online
View Journal | View Issue



Cite this: RSC Adv., 2024, 14, 2610

# One-drop chemosensing of dapoxetine hydrochloride using opto-analysis by multichannel µPAD decorated silver nanoparticles: introducing a paper-based microfluidic portable device/sensor toward naked-eye pharmaceutical analysis by lab-on-paper technology†

Farnaz Bahavarnia, ‡ Fereshteh Kohansal ‡ and Mohammad Hasanzadeh \*\* \*\*

Dapoxetine (DPX) belongs to the selective serotonin reuptake inhibitor (SSRI) class and functions by blocking the serotonin transporter and increasing serotonin activity, thereby delaying ejaculation. Therefore, monitoring of the concentration of DPX in human biofluids is important for clinicians. In this study, application of silver nanoparticles with the morphology of prisms (AqNPrs) for the sensitive measurement of DPX using colorimetric chemosensing and the spectrophotometric method was investigated. Also, DPX was determined in real samples using the spectrophotometry method. Based on the obtained results, all of the detection process in colorimetric assay is related to morphological reform of AqNPrs after it's specific electrostatic and covalent interaction with DPX as analyte. The UV-vis results indicate that the proposed AqNPrs-based chemosensing system has a wide range of linearity (0.01 µM to 1 mM) with a low limit of quantification of 0.01 μM in human urine samples, which is suitable for clinical analysis of this drug in human urine samples. It is important to point out that, this chemosensing strategy showed inappropriate analytical results for the detection of DPX in human urine samples which is a novelty of this platform. Finally, the optimized microfluidic paper-based analytical device (µPAD) was integrated with the colorimetric analysis of DPX to provide a time/color system for estimating analyte concentration by a portable substrate toward in situ and on-site biomedical analysis. Interestingly, the analytical validation tests showed appropriate results with great stability, which may facilitate commercialization of the engineered substrate. For the first time, in order to provide a simple and portable colorimetric/spectrophotometric recognition system to sensitive determination of DPX, an optimized pump-less microfluidic paper-based colorimetric device (µPCD) was introduced and validated for the real-time biomedical analysis of this analyte. According to the obtained results, this alternative approach is suitable for therapeutic drug monitoring (TDM) and biomedical analysis by miniaturized and cost-beneficial devices

Received 4th October 2023 Accepted 8th January 2024

DOI: 10.1039/d3ra06752a

rsc.li/rsc-advances

## 1. Introduction

One of the most common causes of mental impairment across populations globally is depression and mood disorders.¹ The pathophysiology of depression is thought to involve a number of elements, including neurobiological, genetic, environmental (stress), and psychological ones, according to a growing corpus

of research.<sup>2,3</sup> Serotonin, noradrenaline, and dopamine levels in synaptic clefts are thought to be out of balance when depressive symptoms start to appear.<sup>4,5</sup>

The first medication initially approved for the on-demand treatment of men with PE (Premature Ejaculation) is dapoxetine hydrochloride (DPX), which belongs to the class of medicines that are called selective serotonin reuptake inhibitors. The DPX causes a delay in ejaculation by blocking the serotonin (5-HT) transporter, which also increases serotonin's activity at the postsynaptic cleft. It is important to point out that, DPX was first developed as an antidepressant and is a selective 5-HT reuptake inhibitor (SSRI). The DPX increases the level of serotonin available in synaptic clefts, which then binds to the serotonin receptors. The mechanism of action of

<sup>&</sup>lt;sup>a</sup>Nutrition Research Center, Tabriz University of Medical Sciences, Tabriz, Iran

<sup>&</sup>lt;sup>b</sup>Drug Applied Research Center, Tabriz University of Medical Sciences, Tabriz, Iran

'Pharmaceutical Analysis Research Center, Tabriz University of Medical Sciences,
Tabriz, Iran. E-mail: hasanzadehm@tbzmed.ac.ir

<sup>†</sup> Electronic supplementary information (ESI) available. See DOI https://doi.org/10.1039/d3ra06752a

<sup>‡</sup> Co-first author.

Paper

DPX is considered to involve the suppression of serotonin reuptake by neurons and the consequent potentiation of 5-HT activity.13 For instance, researchers14 showed that the application of DPX in PE therapy also consolidated targeted treatments of the brain areas important for sexual behavior, the thalamus and hypothalamus.13

DPX is quickly absorbed and removed from the body, in contrast to other SSRIs. Due to its quick-acting nature, it is effective in treating PE.7 So, DPX has lately been researched as a potential assistance to one method to depression therapy centered on stress reduction, based on an animal model of depression, even though it was first deemed to be ineffectual in its intended use as an antidepressant.8 Numerous approaches such as HPLC and LC/MS have been utilized for the quantification of DPX in pharmaceutical formulations. 15-18 Majority of previous reports referred to measurement of DPX in pharmaceutical products. So, it is necessary to develop sensitive analytical method for determination of DPX in human biofluids like plasma and urine sample. It should be noted that chromatographic methods have commonly employed for the determination of DPX in biofluids, but, this method suffer from drawbacks such as high costs, time-consuming processes, complex instrumentation, and the use of environmentally toxic solvents. 19,20 So, we need sensitive and reliable methods for the rapid and low-cost monitoring of DPX in human real samples.

Colorimetric techniques integrated with spectrophotometric methides like UV-vis, possess high appeal due to their ability to yield easily interpretable detection outcomes visible to the nakedeye. Additionally, these methods exhibit significant advantages such as simplicity, swiftness, cost-effectiveness, and the absence of necessity for complex instrumentation.21 Application of advanced nanomaterials for the colorimetric detection of small molecules play a critically important role as a category of analytical devices, providing chemical insights on diverse subjects such as molecular structure, microscopic imaging, and analyte concentration.<sup>22</sup> Colorimetric-based optical sensors employ a range of signal transduction techniques grounded in photonic properties, encompassing reflectivity, polarization, refractive index, fluorescence intensity, transmission, and absorbance.22

Recently, UV-vis spectrometric method utilizing noble metal nanoparticles have garnered considerable attention due to their distinctive capacity to discern and sensitively manipulate specific analytes among intricate matrices.23 Metal nanoparticles, for instance, AuNPs and AgNPs, serve as colorimetric indicators owing to their optical properties.24-26 Among these anisotropic noble metals, triangular silver nanoprisms (AgNPrs) with plate-like morphology exhibit interesting optical, electrical, and structural characteristics.<sup>24</sup> Anisotropic NPs can also be employed for the colorimetric detection of numerous analytes since their transformation ability.27-33 The presence of three distinct sharp vertices in triangular silver nanoprisms (AgNPrs) renders these metallic nanoparticles inherently unstable as a consequence of their elevated surface energy influenced by the Gibbs-Thomson effect.34

Interestingly, stabilization of AgNPrs on the surface of various substrate led to preparation of novel portable tools for the in situ recognition of a different targets like drugs and biomarkers. One of these tools is microfluidic paper-based analytical devices (μPADs) which have gained significant interest for various analytical and bioanalytical studies.23,35 These devices require hydrophobic barriers on their surfaces to specify fluid flow patterns. Several techniques, such as laser cutting, wax printing, screen printing, and PDMS plotting, can be used to create these hydrophobic barriers.36 The traditional microfluidics, which use expensive materials and cleanroom facilities, can be replaced with paper-based microfluidics that are cost-effective and do not require sophisticated equipment. On the other hand, paper-based sensors have been explored with different monitoring methods, including colorimetric,37 mass spectrometric,38 electrochemical,39 and chemiluminescence techniques. 40 Among them, μPADs-based colorimetric sensors are particularly favored due to their portability and ease of detection.41 The identification of the target substance using colorimetric sensors relies on the alteration of color resulting from the interaction between the signal and the analyte. Numerous researchers have proposed a colorimetric approach that analyzes the color values in photographs to enhance detection accuracy without the need for bulky equipment. 35,42-44

In this study, we described a nano-plasmonic based recognition strategy for colorimetric and spectrophotometric detection of DPX based on AgNPrs. For the first time, a µPAD was decorated with silver nano prisms (AgNPrs) and utilized for the monitoring of DPX in human biofluids. Additionally, DPX was subjected to a quantitative analysis using UV-vis method without needing additional reagents or pre-treatment. The objective of this study was to investigate the colorimetric response of DPX in the presence of different interferer species towards suggestion of a different strategy for the rapid, sensitive and elective sensing of this analyte in real samples. The AgNPrs allowed for suitable selectivity of DPX detection by naked-eye in the presence of other interferer species. Using of µPAD decorated with AgNPrs, the ultimate objective of this study was obtained by providing an appropriate portable tool for the colorimetric identification of DPX in human biofluids.

#### Experimental 2.

## 2.1. Chemical and reagent

Silver nitrate (AgNO<sub>3</sub>), silver chloride (AgCl), PVP K-30 (polyvinyl pyrrolidone), sodium borohydride (NaBH<sub>4</sub>, 96%), hydrogen peroxide (H<sub>2</sub>O<sub>2</sub>, 30 wt%), and tri-sodium citrate (Na<sub>3</sub>C<sub>6</sub>H<sub>5</sub>O<sub>7</sub>) were purchased from Sigma-Aldrich (Canada). Cysteine (Cys), aspartic acid (Asp), arginine (Arg), glucose (Glu), phenylalanine, tyrosine, methionine, proline, and glycine, were obtained from Merck (Germany). The standard solutions of Na<sup>+</sup>, K<sup>+</sup>, Zn<sup>2+</sup>, Mg<sup>2+</sup>, and Ca<sup>2+</sup> were provided by a Chem Lab Company (Zedelgem, Belgium). DPX was provided by Sobhan Darou Company. Glass fiber papers were supplied from Schleicher & Schuell GmbH, Germany (Ref. No. 10 370 55 and Lot No. FL 091-1). Paraffin was prepared from a local market.

## 2.2. Instrumentation

A Shimadzu UV-1800 UV-vis spectrophotometer with 1 nm resolution was used to measure absorbance. The creation of silver nanoprisms was confirmed by using a transmission electron microscope (TEM, Adelaide, Australia), with a 200 kV. To analyze the size dispensation and recognize the zeta potential of the manufactured silver nanoparticles, we used Zetasizer Ver. 7.11 (Malvern Instruments Ltd, MAL 1032660, England) for dynamic light scattering (DLS) analysis. High-resolution field-emission scanning electron microscopy (FE-SEM; Hitachi-Su8020, Czech Republic) with an operating voltage of 3 kV was used to examine the surface geometry of the silver nanoprisms. A Nanosurf (AG, Liestal, Switzerland) device in tapping mode was used to obtain AFM. All of the photographs and videos (see ESI Videos 1–5†) in this work were taken with the smartphone camera. The images were recorded from natural light sources.

### 2.3. Synthesis and characterization of AgNPrs

AgNPrs were synthesized and characterized by based on our previous report.<sup>43</sup>

## 2.4. Paper-based microfluidic device fabrication

In this work, to evaluate the efficiency/suitability of papers, fiber-glass and TLC paper were tested, the results showed that fiberglass paper has less attrition due to better low. Paraffin was used as appropriated wax because of its benefits, including its low melting point, inexpensive cost, and thermoplastic characteristics. Furthermore, paraffin, a key ingredient in solid, is frequently employed in the production of µPAD in the wax printing method and is resistant to the majority of the chemical compounds used in the study. Standard µPAD were constructed via wax printing. 45,46 The proposed pattern consists of eight hydrophilic circular zones. The prepared paper-based template has various microchannels that have a capillary low and the liquid can pass through it easily. The designed microfluidics can utilize to the analysis of several samples simultaneously using different prepared channels and detection zones. In this work, the wax is melted at a temperature of 90 °C, and then the appropriate paper is floated in it for 30 seconds. After drying, the iron pattern was heated for two minutes at 150 °C. A sheet of paper is placed between the iron design and the magnet. As a result, the paraffin penetrated the paper structure and created hydrophilic channels on the surface. The prepared  $\mu PAD$  after drying was utilized for the colorimetric analysis. To decorate the detection zones, a drop of the optical probe was immobilized on the zone and dried at room temperature. 47,48 Therefore, the proposed method is a step towards the development of DPX diagnostic kits that are qualitatively superior and can be rapidly and cheaply recolored. 47 Scheme S1 (see ESI)† shows applied strategy for the construction of μPAD.

## Results and discussion

# 3.1. Detection of DPX by colorimetric and spectrophotometric (UV-vis)

Triangular AgNPrs have an extreme degree of anisotropy and exhibit unique UV-vis wavelengths. Upon addition of DPX, at

the initial moment, the color of these triangular AgNPrs changed from blue to orange, depending on the extent of etching, as shown in Fig. 1. As so as shows that the absorption wavelength of AgNPrs changed after 60 min from 623 to 607 nm with the addition of DPX, accompanied by a subtle color change. According to the obtained results, the maximum absorption intensity of DPX + AgNPrs changed from 1.598 (a.u.) to 0.283 (a.u.) after 60 min. It has changed with the addition of DPX, which is accompanied by a subtle color change process (orange  $\rightarrow$  pale pink).

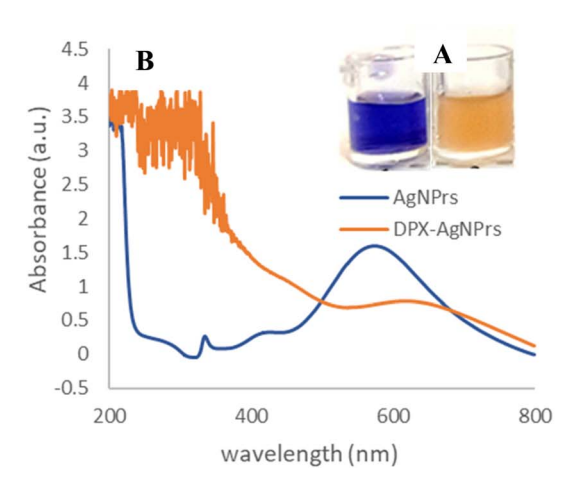
Also Scheme 1 show all of sensing procedure of DPX using engineered colorimetric process.

Triangular AgNPrs have an extraordinary degree of anisotropy and show one of a kind LSPR highlights with a tall termination coefficient. Upon expansion of DPX, the morphology of these triangular AgNPrs changed to circular nanodisks and the color changed from blue to yellow, depending on the degree of carving. Moreover, the UV-vis spectra of the triangular AgNPrs display wide highlights with three unmistakable groups at 335 nm, 475 nm, and 750 nm, which compare to the out-of-plane quadrupole, inplane quadrupole, and in-plane dipole plasmon reverberation of the triangular AgNPrs, individually. The in-dipole reverberation top at 750 nm is amazingly touchy to the thickness and edge length of triangular AgNPrs. As anticipated, the wide crest at 750 nm, which compares to the inplane dipole reverberation, vanished taking after the expansion of DPX, whereas the escalated of the top at 480-500 nm was slowly expanded (Fig. 1). These comes about demonstrate that location of DPX with this triangular AgNPrs test is amazingly touchy to the nanoprism shape versus the top position of the in-plane dipole reverberation.

## 4. Analytical study

To study the concentration effect of DPX by colorimetric and UV-vis methods, various concentrations of DPX (0.01 μM to 1 mM) were prepared in deionized water. Then, AgNPrs were added with a 1:1 v/v ratio. These mixtures were photographed immediately, (0 min) and after 60 min (complete reaction). In the incubation time = 0 minutes after mixing of optical probe with analyte in the concentration range of 10, 5, 1, 0.5, and 0.01 mM of DPX had begun to change the blue color of the AgNPrs which shows initiation of reaction. Interestingly, after 60 minutes, the color of solutions changed as; pale pink for 10 mM, milky for 5 mM, pale blue for 1 mM, pale purple for 0.5 mM, and pale purple for 0.01 mM concentrations of analyte which confirm completion of reaction. The results show that the effect of DPX on AgNPrs not only depends on its concentration but that reaction time is also a key factor. Based on this result, the presence down to a minimum concentration of 10, 5, 1, 0.5, 0.01 mM of DPX in a standard solution would be easily distinguishable by the naked-eye (Fig. 2). The second part of this study was allocated to recording of the UV-vis spectra of standard samples in incubation time of 60 minutes after mixing of analyte with AgNPrs owing to the fact that their color at this point remained nearly

Paper



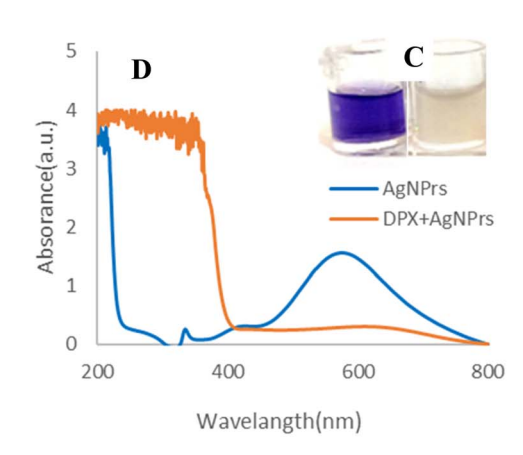
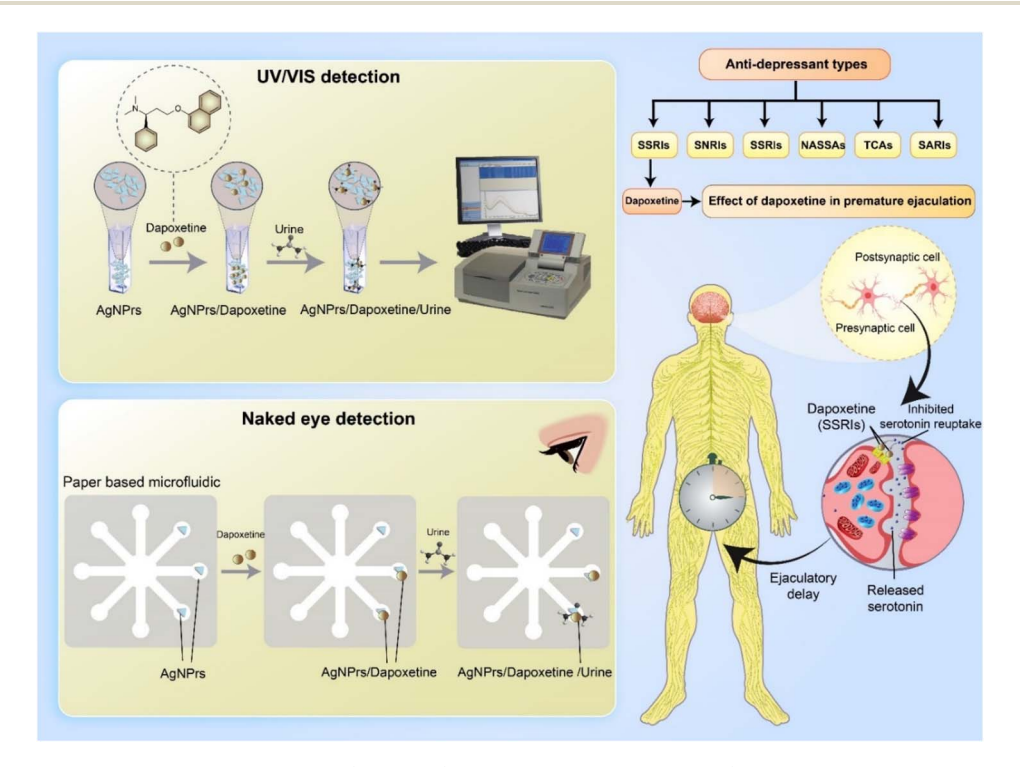


Fig. 1 (A) Assessment of the change in AgNPrs color before and after interaction with DPX (before and after reaction with probe in 0 min). (B) UV-vis spectra of AgNPrs, and AgNPrs-DPX. (C) Assessment of the change in AgNPrs dye before and after interaction with DPX (before and after reaction with DPX (before and after reaction with probe in 60 min). (D) UV-vis spectra of AgNPrs, and AgNPrs-DPX. Labels A&B are related to incubation time = 0 min (immediately after interaction).

stable. As shown in Fig. 2B and D, DPX with concentrations of 10, 5, 1, 0.5 mM, 0.0001 mM has the capability of shifting the spectrum of the absorption band substantially. Subsequently, to evaluate the analytical performance of the method for DPX detection, under the optimized conditions, different concentrations of DPX are added to AgNPrs, as illustrated in Fig. 2A and B the change of the maximum wavelength of AgNPrs ( $\Delta I$ ) decreases and the color shows less change with the increase of DPX concentration, which is ascribed to the

better protection effect of DPX. Thus, the concentration of the DPX was quantified based on the relationship between the concentration of DPX and  $\Delta I$ . As shown in Fig. 2E and F, suitable linear relationship between  $\Delta I$  and DPX concentration ranging from 0.01  $\mu$ M to 1 mM is observed. The linear regression equation is  $\Delta_{\rm abs} = 1.1722 \log C_{\rm DPX} + 0.8642$  (in 0 min),  $\Delta_{\rm abs} = 0.9157C_{\rm DPX} + 0.0163$  (in 60 min) with a linear coefficient of 0.8716 in incubation time = 60 min. The detection limit is as low as 0.01  $\mu$ M.



Scheme 1 A visual representation depicting the identification of dapoxetine in real samples of urine, using UV-visible spectroscopy and  $\mu$ PAD colorimetric assay.

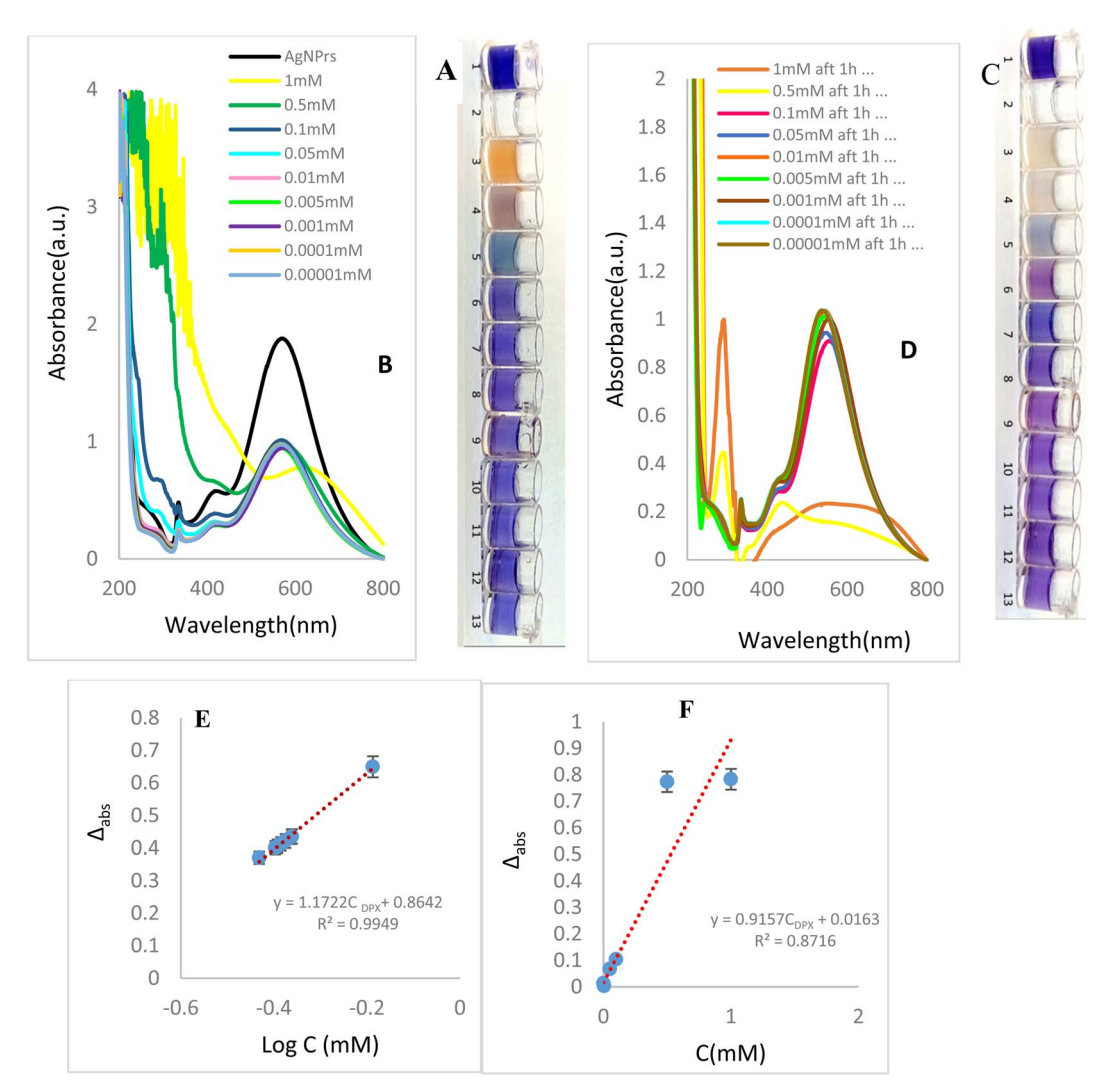


Fig. 2 (A) Colorimetric sensing of various concentrations of DPX by AgNPrs at incubation time = 0 min (the ratio was 1:1 v/v). (B) UV-vis spectra of different concentrations of DPX with AgNPrs at a 1:1 ratio in 0 min. (C) Colorimetric sensing of AgNPrs spiked with DPX of various concentrations at 60 min (the ratio was 1:1). (D) The UV-vis spectra of different concentrations of DPX with AgNPrs at a 1:1 v/v ratio incubation time = 60 min). (E) The linear relationship between shift of  $\lambda$  and the concentration of DPX ranging from 1 to 0.00001 mM (left to right)  $\Delta I = (I_{\text{(AgNPrs)}} - I_{\text{(C)}})$ , denotes of  $\Delta$ (abs) according to concentration or logarithm of concentration of AgNPrs with DPX in 0 min. (F) The linear relationship between shift of  $\lambda$  and the concentration of DPX ranging from 1 to 0.00001 mM (left to right)  $\Delta I = (I_{\text{(AgNPrs)}} - I_{\text{(target)}})$ , denotes of  $\Delta$ (abs) according to concentration or logarithm of concentration of AgNPrs with DPX in 60 min. The reason of this approach is related to different change the morphology of AgNPrs in the presence of different concentration of DPX in various incubation time. The three absorption bands can be assigned to out-of-plane and in-plane quadrupole resonance and in-plane dipole resonance of AgNPrs, respectively. Furthermore, the peak of the in-plane dipole resonance is highly shape dependent, which is utilized to design wavelength alterations-based sensors. With the addition of DPX, a blue shift of the in-plane dipole resonance peak in the LSPR spectra and color change of the solution from blue to yellow was observed. These phenomena are attributed to the morphology transformation of AgNPrs and the tendency of newly generated Ag atoms to deposit on the surface of AgNPrs. Thus, the wavelength shift of the in-plane dipole resonance peak of AgNPrs was used for the determination of DPX.

## 4.1. Real sample analysis

The reported colorimetric and spectroscopic approaches were also used to determine of DPX in human urine samples. For this purpose, DPX was spiked in the human urine sample and mixed with AgNPrs as optical probe in a 1:1 v/v ratio and 1:0.5:0.5 v/v/v ratio. Then, they were analyzed by colorimetric and spectroscopic methods. According to the obtained results indicated in Fig. S1 (see ESI),† after 60 min incubation of abovementioned materials, the color of the mixture changed to

dark grey. So, the AgNPrs probe can recognize DPX in human urine samples. The color of the mixture to dark grey. The AgNPrs probe can recognize DPX in urine. The AgNPrs probe can recognize DPX in urine.

Also based on the UV/vis graph, at the wavelength of 571.5 nm, the absorption rate corresponding to the sample of urine + DPX + probe is 0.437 (a.u.), which is an acceptable result, and in terms of the location of the wavelength, it is exactly consistent with the spectrum of AgNPrs. It is worth mentioning that the colorimetric identification in the urine sample was

Paper RSC Advances

done at room temperature. As shown in the UV/vis, after the addition DPX-probe mixture to the human urine samples, the peak intensity at 571.5 nm decreased from 0.1446 (a.u.) to 0.437 (a.u.) which confirmed interaction of optical probe with the analyte in real sample. Therefore, the AgNPrs probe can detect DPX in human urine samples.

## 4.2. Selectivity analysis

Selectivity is one of the important aspects was evaluated by performing the assessment in the presence of other species in real samples. The prepared AgNPrs colloidal solution was sea blue and started to change color as soon as drug solutions were added. As previously mentioned, eight different drugs, namely codeine phosphate, caffeine anhydrous, pantoprazole, DPX, levofloxacin, ciprofloxacin, donepezil, and cholesterol introduced into AgNPrs standard solution at a 1:1 v/v ratio to induce distinct color changes for analyte detection. As shown in Fig. 3, there is a clear color change for AgNPrs. As soon as the DPX solution was added to AgNPrs, its color changed from sea blue to dark grey color. Interestingly, after an hour the color of the mixture had changed to a light grey color. The rest of the analyzed drugs did not change significantly after being added to AgNPrs. On this basis, DPX can be detected by proposed

colorimetric system in the presence of other drugs with similar structure. So mentioned drugs have no interfering effect on the monitoring of DPX.

All of the obtained results by colorimetric assay were confirmed by UV/vis. The ready AgNPrs colloidal solution was sea blue as soon as the yellow solution of DPX (10 mM) was added, the color changed to dark grey. After 60 minutes, the color of the mixture became lighter than at 0 minutes. UV-vis spectra and the histogram curve of peak intensity *versus* AgNPrs, DPX, and other drugs including (codeine phosphate, caffeine anhydrous, pantoprazole, levofloxacin, donepezil, ciprofloxacin) at different time intervals are shown in Fig. S2 and S3 (see ESI).† For DPX, LSPR peaks were recorded at 514 nm for 0 minutes and LSPR peaks at 767.5 nm for 60 minutes. Therefore, these absorption bands were confirmed for AgNPrs. The selectivity of the AgNPrs-based approach for the detection of DPX was evaluated by monitoring the change in the maximum absorption wavelength of AgNPrs.

By spiking the AgNPrs solution with DPX, the intensity of the solution bands decreased significantly. The biggest shift for this band occurred in 60 minutes at 767.5 nm. In addition, after spiking the AgNPrs solution with DPX, which is shown in Fig. S3 (see ESI).† The satisfied selectivity is mainly attributed to the

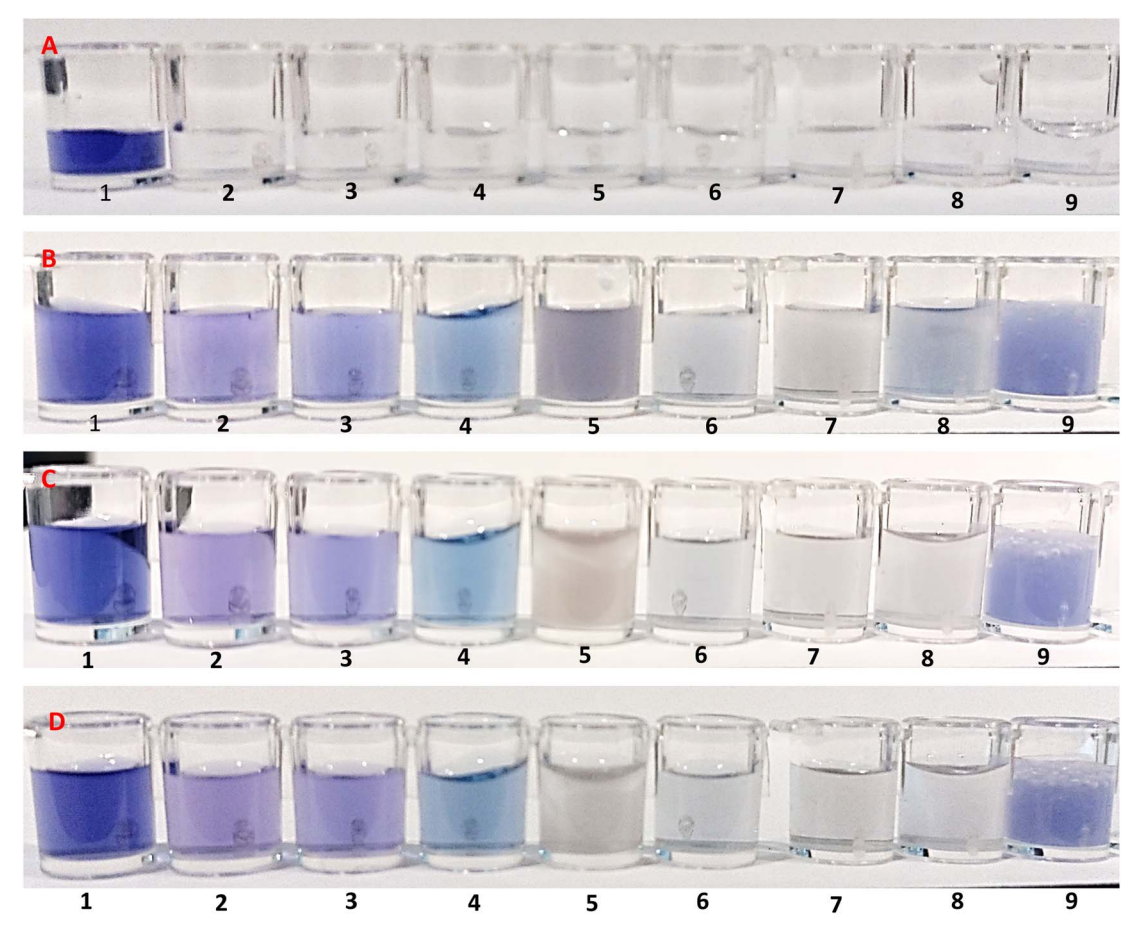


Fig. 3 (A) Photographic images of (1) AgNPrs, (2) codeine phosphate, (3) caffeine anhydrous, (4) puntoprazole, (5) DPX, (6) levofloxacin, (7) ciprofloxacin, (8) donepezil, (9) cholestrol (10 mM in DI water), (B) after adding 100  $\mu$ L of AgNPrs with 1:1 v/v ratio, (C) 30 min after reaction, (D) 1 h after reaction.

high affinity binding between DPX and AgNPrs via Ag-catechol bonds.

In order to verify the selectivity of the proposed method, the effects of some common inorganic ions and amino acids were investigated.

At this point, 10 mM solutions of K<sup>+</sup>, Na<sub>2</sub>NO<sub>3</sub>, Ca<sup>2+</sup>, Zn<sup>2+</sup>, glycine (Gly), phenylalanine (Phe), arginine (Arg), tyrosine (Tyr), proline, histidine, glutamine, methionine, ciprofloxacin, donepezil, levofloxacin, codeine phosphate and pantoprazole, in 1:1 v/v ratio were mixed with AgNPrs (as optical probe) and DPX solution (as analyte) and the results were compared to a DPX/probe mixture under the same conditions to detect if interfering agents has significant effect on the optical sensing of DPX [Fig. S4 and S5 (see ESI)].† Since the etching effect of DPX and other similar species on AgNPrs depends on reaction time, the time for examination was set to 0 and 60 min after mixing the components. While other mixtures changed the color to a lighter shade, the obtained data revealed the high selectivity of AgNPrs toward DPX in the first minute of reaction. For the better investigation, 50 µL of DPX was combined with 50 µL of interferential species (10 mM). Then, 100 µL of AgNPrs (optical probe) was added to the DPX/interference mixture and colorimetric tests were performed. At the same initial moment, since the addition of metal ions, the blue color of AgNPrs changed to yellow. Also, in the process of arginine the color of optical probe was changed. But, the other amino acids tyrosine, alanine, and glycine were recorded in blue color, after 60 minutes it became lighter. Also, the amino acid arginine appeared in dark purple color at first and changed to pale purple color after 60 minutes. According to the results, the selectivity of the interaction of amino acids with DPX is such that both at 0 min and at 60 min, amino acids are able to assist for suitable (high resolution) detection of the analyte (DPX). So, amino acids, especially arginine, are able to assist to identify the analyte by candidate optical probe (AgNPrs). For this reason, arginine has suitable effect on the appropriate monitoring of DPX. While metal ions alone have to interfering, behavior identify the analyst. It should be noted that different concentrations of DPX with urine and arginine were investigated which no significant change was observed on the colorimetric tests. It is important to point out that the colorimetric assay of DPX in the presence of some ions and amino acids showed no significant change that occurred in the colorimetry analysis of this candidate analyte.

## 4.3. Repeatability and reproducibility

Repeatability of the tests was assessed over a 3 day period using three distinct concentrations (high, medium, low) of DPX solution, measured at different incubation times (0 and 60 minutes), and the findings were presented in terms of Relative Standard Deviation (RSD). As depicted in Fig. S6 (see ESI),† the UV-vis spectrum results reveal minimal alterations in the three absorption bands. While the intensity of these bands decreased gradually, the reduction ratio remained consistent across all of them, with no impact on their wavelength positions. Thus, these findings affirm the validity of the tests in the term of repeatability.

The information presented in the Table S1 (see ESI)† indicates UV-vis spectra measurements taken at different concentrations of a substance on three consecutive days, both at 0 minutes (immediately) and 60 minutes after the initial measurement. Here's an interpretation:

The standard deviation (SD) values represent the amount of variation or dispersion in the measurements for each concentration level and time point. Here's how to interpret them:

- (1) SD for 0 minutes:
- $\bullet$  0.5 mM: the SD is approximately 10.50. This means that the measurements at this concentration on the first day had a moderate amount of variation around the mean wavelength of 573 nm.
- 0.01 mM: the SD is about 1.80. This indicates a low level of variation in measurements around the mean wavelength of 571.5 nm on the first day.
- 0.00001 mM: the SD is roughly 1.53. Similar to the 0.01 mM concentration, this suggests a low level of variation around the mean wavelength of 570 nm on the first day.
  - (2) SD for 60 minutes:
- 0.5 mM: the SD is approximately 9.64. This shows a moderate amount of variation around the mean wavelength of 559 nm at the 60 minute mark.
- 0.01 mM: the SD is about 2.89. This indicates a slightly higher level of variation in measurements around the mean wavelength of 550 nm at 60 minutes.
- 0.00001 mM: the SD is roughly 2.84. Similar to the 0.01 mM concentration, this suggests a somewhat higher level of variation around the mean wavelength of 551.5 nm at 60 minutes.

Table 1,<sup>49-55</sup> indicated analytical results of different reports for the detection of DPX as can be seen, various biomedical methods such as HPLC-MS, HPLC-MS/MS, LC-MS/MS, spectrophotometric, fluorometric, UPLC-MS, UPLC-MS/MS, have been utilized for the monitoring of DPX.

Although, previous reports show excellent analytical data for the defemination of DPX, but there are some limitations such as various treatment process, complicated mobile phases, and time-consuming extraction procedures with restricted applicability. A comparison of the results obtained in this study with previously reported works shows that the developed method has some advantages over previous approaches, such as no need for pre-treatment of samples, no need for a professional operator, no need for long measurement time, the analysis process is done in the form of on-site analysis, ability to analyze models using smartphones, not using large data, and comparison of content analysis results. Interestingly, for the first time, recognition of DPX in human urine sample was performed using proposed spectrophotometric method. So, a noninvasive method was developed for the monitoring of DPX in human biofluids which is main advantages of the suggested strategy. On the other hand, due to simple matric of human urine sample (minor number of interfering species) the recognition process can done easily which is another advantage of this method than other reports.

Table 1 The analytical performances of various methods for the identification of DPX

Method	Nano probe, nano-polymer	LLOQ	Linear range	Samples	Ref.
HPLC/MS	0.01 M ammonium acetate + 0.02% formic acid solution	5.0 ng mL <sup>-1</sup>	5.0-600 ng mL <sup>-1</sup>	Human plasma	49
Principal component analysis (PCA) and continuous wavelet transform (CWT) combined with UV-vis spectrophotometry	NA	$1.169~\mu g$ $mL^{-1}$	NA	Pharmaceutical samples	50
HPLC-MS/MS		$2~{\rm ng~mL}^{-1}$	2.00–1000 ng mL <sup>-1</sup>	Human plasma	51
LC-MS/MS		$10 \text{ ng mL}^{-1}$	10-6000 ng mL <sup>-1</sup>		52
Spectrophotometric and spectrofluorometric		$0.71 \ \mu g \ mL^{-1}$	$2.0-20.0 \ \mu g \ mL^{-1}$	NA	53
UHPLC/MS	0.5% formic acid/acetonitrile (60:40, v/v)	$1~{\rm ng~mL^{-1}}$	1-500 ng mL <sup>-1</sup>	Rat plasma	54
UHPLC-MS/MS	A mobile phase of acetonitrile and 0.1% formic acid in water	1.0 ng mL <sup>-1</sup>	1.0-200 ng mL <sup>-1</sup>	Human plasma	55
μPAD integrated spectrophotometry	AgNPrs	0.01 μΜ	0.01 $\mu M$ to 1 $mM$	Human urine	This work

# 4.4. Naked-eye colorimetric assay of DPX using one-droplet paper-based microfluidic system (OD-μPAD)

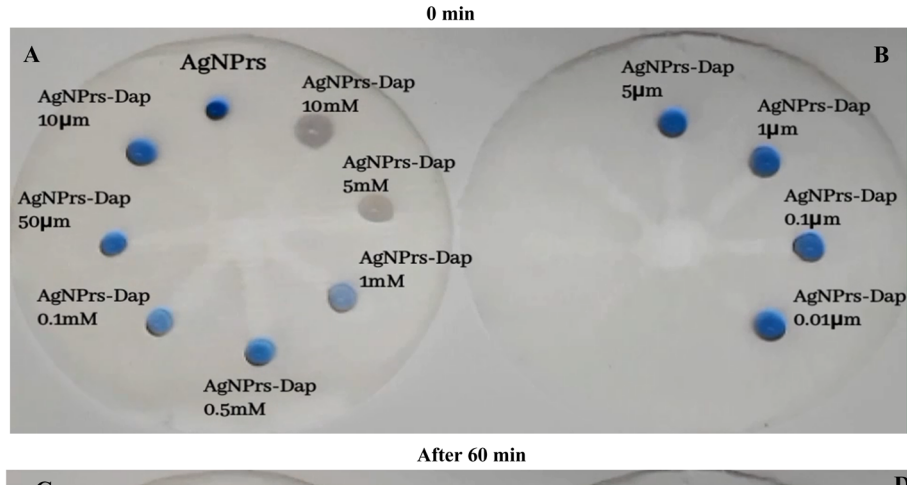
Based on obtained results in colorimetric/spectrophotometric study of DPX, in this part of study, a portable was substrate for the in situ monitoring of this analyte. This tool can be used for the real time analysis of DPX. In this study μPAD was engineered using stabilizing of optical probe on the surface of multichannel of rebar glass. So, two kinds of uPAD, were prepared and underwent examination. In the first attempt, the microfluidic network was established with 20 seconds of heat and pressure on the fiberglass paper. The hydrophilic network of prepared microfluidic paper was very permeable towards AgNPrs and DPX. As soon as AgNPrs and DPX were injected, they were absorbed in the paper. So, no significant color change occurred in the injected areas' protection zone. In a second attempt, the time of exposure to molten wax was increased to 30 second subsequently, the hydrophilic network changed to a semi hydrophobic one which was more resistant to absorption of AgNPrs and DPX. As can be seen in Fig. 4, after 5 minutes the concentrations of 1 and 5 mM showed a significant color change from purple to pink. After approximately 30 minutes of reaction time, the injection drops of AgNPrs and DPX were adsorbed or dried on the paper (see Video files in ESI†), and after 60 minutes as indicated in the figure, in addition to the previous concentrations that included 1 mM, 5 mM and half mM, concentrations of 0.1 mM and 0.05 mM also led to change of color to pale pinkish (see Fig. 4 and Video (see ESI†)).

For the analytical studies by  $\mu PADs$ , all of engineered zones were decorated by AgNPrs. Then, different concentrations of DPX were adding to the zones, for better results various incubation times loading were adopted, wells no. 2 to no. 8 were injected with 5 mL of different concentrations of DPX (10, 5, 1, 0.5, 0.1 mM and 1, 50, 10, 5, 1, 0.1, 0.01  $\mu$ M), after adding 5 mL of freshly prepared AgNPrs into all wells. Also, after 30 min of incubation time, the color change was evident in 1 mM, and 0.5 mM concentrations of DPX. After 60 minutes of the reaction

time, the color of mixture was changed which confirmed complete of reaction of probe with analyte and determination was done successfully. It is important to point out that, the proposed subsided is able to default high concentration of this analyte (1–50  $\mu$ M). It is important to point out that, very low concentration of DPX can't determine by this  $\mu$ PAD (see video (see ESI†)). So, we need to optimize the surface/time/heat/viscosity of  $\mu$ PAD toward ultra-sensitive monitoring of DPX by these kinds of devices.

For the specificity analysis of engineered substrate for the selective detection of DPX, the effect of potential interferers, Gly, Tyro, Arg, Phe, pantoprazole, ciprofloxacin, donepezil, levofloxacin, codeine phosphate, and dopamine, in 1:0.5:0.5 v/v/v ratio and with potential ions of  $K^+$ ,  $Na^+$ ,  $Ca^{2+}$ , and  $Zn^{2+}$ , in 1:1 v/ v volume ratio on the colorimetric performace of μPADs were evaluated. As shown in Fig. S10-S12 (see ESI†), 10 μL of AgNPrs was injected into each well of µPAD from no. 1 to no. 8. Afterward, 5 µL of DPX (0.5 mM) and interferers 10 mM was added to wells no. 2 to no. 8. After 60 min, the color change of the wellcontaining interferer Ca2+, Zn2+, arginine is quite tangible, while the other wells did not show any noticeable color change. The obtained results indicate that none of these species can interfere with DPX at the same concentration. Nevertheless, at concentrations of 10 mM of arginine, turning the hue of AgNPrs to grey, Ca<sup>2+</sup>, and Zn<sup>2+</sup> by turning the hue of AgNPrs to pink after one hour, can be considered an interferer [Fig. S7 and S8 (see ESI)].† However, we also investigated the interactions separately for DPX and with various types of potential interferers, (Gly)/(Tyro)/(Arg)/(Phe)/and potential ions K<sup>+</sup>, Na<sup>+</sup>, Ca<sup>2+</sup>, Zn<sup>2+</sup>, and recorded the results for different times. According to the obtained results, in different incubation times, no color changes occurred at various incubation times (see Video files in ESI†).

It is important to point out that, main novelty of the present study is the use of the colorimetric  $\mu$ PAD integrated spectrophotometry procedure for the determination of DPX in human



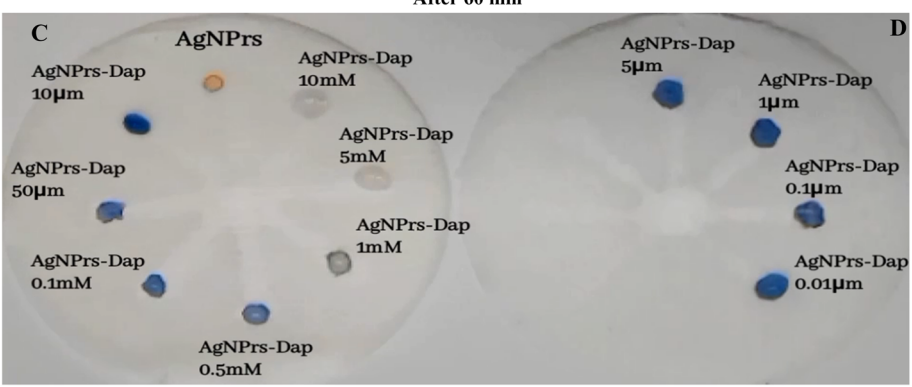


Fig. 4 (A) Photographic images of the fiberglass microfluidic paper-based colorimetric chemosensor after 5 min, with different concentrations of DPX. (1) AgNPrs without DPX, (2) DPX, (3) AgNPrs, 10 mM DPX, (4) AgNPrs, 5 mM DPX, (5) AgNPrs, 1 mM DPX, (6) AgNPrs, 0.5 mM DPX, (7) AgNPrs, 0.1 mM DPX, and (8) AgNPrs, 50 μM DPX, (9) AgNPrs, 10 μM DPX, (10) AgNPrs, 5 μM DPX, (11) AgNPrs, 1 μM DPX, (12) AgNPrs, 0.1 μM DPX, (13) AgNPrs, 0.01 μM DPX. (8) Photographic images of the fiberglass microfluidic paper-based colorimetric chemosensor after 30, min, with different concentrations of DPX. (1) AgNPrs without DPX, (2) DPX, (3) AgNPrs, 10 mM DPX, (4) AgNPrs, 5 mM DPX, (5) AgNPrs, 1 mM DPX, (6) AgNPrs, 0.5 mM DPX, (7) AgNPrs, 0.1 mM DPX, and (8) AgNPrs, 50 μM DPX, (9) AgNPrs, 10 μM DPX, (10) AgNPrs, 5 μM DPX, (11) AgNPrs, 1 μM DPX, (12) AgNPrs, 0.1 μM DPX, (13) AgNPrs, 0.01 μM DPX. (C and D) Photographic images of the fiberglass microfluidic paper-based colorimetric chemosensor after 60 min, with different concentrations of DPX. (1) AgNPrs without DPX, (2) DPX, (3) AgNPrs, 10 mM DPX, (4) AgNPrs, 5 mM DPX, (5) AgNPrs, 1 mM DPX, (6) AgNPrs, 0.5 mM DPX, (7) AgNPrs, 0.1 mM DPX, (10) AgNPrs, 50 μM DPX, (9) AgNPrs, 10 μM DPX, (10) AgNPrs, 5 μM DPX, (11) AgNPrs, 1 μM DPX, (12) AgNPrs, 0.1 μM DPX, (13) AgNPrs, 0.01 μM DPX, (13) AgNPrs, 0.01 μM DPX, (14) AgNPrs, 0.01 μM DPX, (15) AgNPrs, 0.01 μM DPX, (16) AgNPrs, 0.01 μM DPX, (17) AgNPrs, 0.01 μM DPX, (18) AgNPrs, 0.01 μM DPX, (19) AgNPrs, 0.01 μM DPX, (19) AgNPrs, 0.01 μM DPX, (10) AgNPrs, 0.01 μ

urine samples which was reported for the first time in this report.

## Conclusions

In summary, utilization of AgNPrs for the optical chemosensing of DPX was evaluated by colorimetric and UV/vis spectrophotometer methods. The obtained analytical results for the proposed AgNPrs-based colorimetric chemosensor are comparable with others, as this colorimetric system enjoys a broad range of linearity of 0.01  $\mu M$  to 1 mM and possesses an appropriate LLOQ of 0.01  $\mu M$ . Moreover, AgNPrs could utilized for the detection of DPX in a human urine sample. In the last part of this work, for the pharmaceutical analysis,  $\mu PAD$  was used as portable device which was engineered based on integration smartphone with paper-based sensor technology towards *in situ* analysis of candidate target drug. This optimization paved the way for offering an innovative analytical method that is based on the time/color

characterization of various concentration of DPX. The selectivity tests for the engineered systems (solution and integrated µPAD) were also appropriate, and the stability of the AgNPrs was confirmed for at least three months, which makes it's patented to commercialization. Apart from the validated colorimetric recognition and UV/vis systems for DPX, an optimized µPAD was proposed toward portable analysis of DPX in real samples. In addition to a basic and sensitive color recognition system for DPX, this research provides an improved method for measuring the absorbance of solutions like AgNPrs on paper, and a unique method for estimating the concentration of substances based on time and color. It is important to point out that, this chemosensing strategy showed inappropriate analytical results for the detection of DPX in human urine samples which is weakness of this platform. Therefore, we can infer that the application of colorimetric and spectrophotometric methods based on AgNPrs has the potential to revolutionize the detection of medicines, paving the way for new possibilities in this field.

## Conflicts of interest

There are no conflicts to declare.

## Acknowledgements

We are grateful for financial assistance for this work from the Tabriz University of Medical Sciences' Pharmaceutical Analysis Research Center (Tabriz, Iran) (Grant No. 72824, IR.TBZMED.VCR.REC.1402.192).

## References

- 1 E. J. Nestler, M. Barrot, R. J. DiLeone, A. J. Eisch, S. J. Gold and L. M. Monteggia, *Neuron*, 2002, 34, 13–25.
- 2 C. A. Hall and C. F. Reynolds III, *Maturitas*, 2014, **79**, 147–152.
- 3 C. Berthou, J. P. Iliou and D. Barba, eJHaem, 2022, 3, 263-275
- 4 N. Sánchez, J. Juárez-Balarezo, M. Olhaberry, H. González-Oneto, A. Muzard, M. J. Mardonez, P. Franco, F. Barrera and M. Gaete, *Front. Cell Dev. Biol.*, 2021, **9**, 632766.
- 5 P. Belujon and A. A. Grace, *Int. J. Neuropsychopharmacol.*, 2017, **20**, 1036–1046.
- 6 M. A. Magdy, B. H. Anwar, I. A. Naguib and N. S. Abdelhamid, *Spectrochim. Acta, Part A*, 2020, **226**, 117611.
- 7 K. E. Andersson, J. P. Mulhall and M. G. Wyllie, *BJU Int.*, 2006, 97, 311–315.
- 8 H. Rafi and M. Farhan, Pak. J. Pharm. Res., 2016, 2(1), 15-22.
- 9 J. Kasper, S. B. Eickhoff, S. Caspers, J. Peter, I. Dogan, R. C. Wolf, K. Reetz, J. Dukart and M. Orth, *Brain*, 2023, awad043.
- 10 J. M. Shine, C. O'Callaghan, I. C. Walpola, G. Wainstein, N. Taylor, J. Aru, B. Huebner and Y. J. John, *Brain*, 2022, 145, 2967–2981.
- 11 R. S. Duman, S. Deyama and M. V. Fogaça, Eur. J. Neurosci., 2021, 53, 126–139.
- 12 P. Ratajczak, K. Kus, T. Zaprutko, M. Szczepański and E. Nowakowska, *Acta Neurobiol. Exp.*, 2019, **79**, 13–24.
- 13 C. G. McMahon, Ther. Adv. Urol., 2012, 4, 233-251.
- 14 P. Clement and F. Giuliano, *Basic Clin. Pharmacol. Toxicol.*, 2016, 119, 18–25.
- 15 H. Gadiya, M. Maheshwari and A. Dashora, *Asian J. Pharmaceut. Clin. Res.*, 2019, **12**, 328–331.
- 16 K. B. Liew and K. K. Peh, Acta Pol. Pharm., 2014, 71, 393-400.
- 17 C. SARIOĞLU and S. SAĞLIK ASLAN, *Lat. Am. J. Pharm.*, 2019, 38(10), 2112–2120.
- 18 K. Kalyani and V. Anuradha, *Der Pharm. Lett.*, 2015, 7, 98-
- 19 N. Vasava, Advantages and Disadvantages of Chromatography, https://www.pharmastuff4u.com/2023/03/advantages-anddisadvantages-of.html.
- 20 E. Ö. Er, B. Özbek and S. Bakırdere, *Measurement*, 2018, **124**, 64–71.
- 21 T. Lou, Z. Chen, Y. Wang and L. Chen, *ACS Appl. Mater. Interfaces*, 2011, 3, 1568–1573.

- 22 T. Khan, https://www.azosensors.com/article.aspx?
  ArticleID=2808.
- 23 S. Ahmadi, Z. Ghasempour and M. Hasanzadeh, *Food Chem.*, 2023, **423**, 136307.
- 24 Y. Wang, Y. Yang, W. Liu, F. Ding, Q. Zhao, P. Zou, X. Wang and H. Rao, *Microchim. Acta*, 2018, **185**, 1–9.
- 25 S. Ahmadi, M. Hasanzadeh and Z. Ghasempour, *Food Chem.*, 2023, **402**, 134501.
- 26 M. Amjadi, T. Hallaj and R. Salari, Sens. Actuators, B, 2018, 273, 1307–1312.
- 27 K. Ghaseminasab, N. Aletaha and M. Hasanzadeh, *RSC Adv.*, 2023, **13**, 3575–3585.
- 28 R. Singh and H. S. Nalwa, *J. Biomed. Nanotechnol.*, 2011, 7, 489–503.
- 29 S. M. Dadfar, K. Roemhild, N. I. Drude, S. von Stillfried, R. Knüchel, F. Kiessling and T. Lammers, *Adv. Drug Deliv. Rev.*, 2019, **138**, 302–325.
- P. Prosposito, L. Burratti and I. Venditti, *Chemosensors*, 2020,
   26.
- 31 N. Faraji and Z. Hajimahdi, *Micro Nano Lett.*, 2018, **13**, 1667–1671.
- 32 H. S. Kim and D. Y. Lee, J. Pharm. Invest., 2017, 47, 19-26.
- 33 C. Liu, Q. Pang, T. Wu, W. Qi, W. Fu and Y. Wang, *J. Anal. Test.*, 2021, 5, 210–216.
- 34 S.-J. Yoon, Y.-S. Nam, H.-J. Lee, Y. Lee and K.-B. Lee, *Sens. Actuators, B*, 2019, **300**, 127045.
- 35 F. Farshchi, A. Saadati, M. Hasanzadeh and F. Seidi, *RSC Adv.*, 2021, **11**, 27298–27308.
- 36 L.-J. Yan, C. Jiang, A.-Y. Ye, Q. He and C. Yao, *Spectrochim. Acta, Part A*, 2022, **268**, 120639.
- 37 M. C. Carneiro, L. R. Rodrigues, F. T. Moreira and M. G. F. Sales, *Sensors*, 2022, 22, 3221.
- 38 Q. Chen, Z. He, W. Liu, X. Lin, J. Wu, H. Li and J. M. Lin, *Adv. Healthcare Mater.*, 2015, **4**, 2291–2296.
- 39 V. B. C. Lee, N. F. Mohd-Naim, E. Tamiya and M. U. Ahmed, *Anal. Sci.*, 2018, **34**, 7–18.
- 40 J. L. Delaney, C. F. Hogan, J. Tian and W. Shen, *Anal. Chem.*, 2011, **83**, 1300–1306.
- 41 P. T. Lin, S. W. Kwok, H.-Y. G. Lin, V. Singh, L. C. Kimerling, G. M. Whitesides and A. Agarwal, *Nano Lett.*, 2014, 14, 231–238.
- 42 L. Liang, S. Ge, L. Li, F. Liu and J. Yu, *Anal. Chim. Acta*, 2015, **862**, 70–76.
- 43 A. Saadati, F. Farshchi, M. Hasanzadeh and F. Seidi, *Anal. Methods*, 2021, 13, 3909–3921.
- 44 A. Manbohi and S. H. Ahmadi, *Environ. Monit. Assess.*, 2022, **194**, 190.
- 45 X. Luo, S. Zhang, Z. Xia, R. Tan, Q. Li, L. Qiao, Y. He, G. Zhang and Z. Xu, *Anal. Chim. Acta*, 2023, **1241**, 340803.
- 46 J. Chen, L. Zeng, T. Xia, S. Li, T. Yan, S. Wu, G. Qiu and Z. Liu, *Anal. Chem.*, 2015, **87**, 8052–8056.
- 47 E. B. Strong, S. A. Schultz, A. W. Martinez and N. W. Martinez, *Sci. Rep.*, 2019, **9**, 7.
- 48 P. Abdollahiyan, M. Hasanzadeh, P. Pashazadeh-Panahi and F. Seidi, *J. Mol. Liq.*, 2021, **338**, 117020.
- 49 R. Said, B. Arafat and T. Arafat, J. Chromatogr. B: Anal. Technol. Biomed. Life Sci., 2020, 1149, 122154.

- 50 M. Ramin, M. R. Sohrabi and F. Motiee, *Chemom. Intell. Lab. Syst.*, 2022, **230**, 104656.
- 51 X. Zhang, Z. Gao, F. Qin, K. Chen, J. Wang and L. Wang, *Molecules*, 2022, 27, 2707.
- 52 M. N. Abou-Omar, A. M. Annadi, N. M. El Zahar, A. O. Youssef, M. A. Amin, M. S. Attia and E. H. Mohamed, RSC Adv., 2021, 11, 29797–29806.
- 53 H. S. Elama, F. A. Elsebaei, F. A. A. Ali and A. M. El-Brashy, *Luminescence*, 2018, 33, 1306–1313.
- 54 T. K. Kim, I. S. Kim, S. H. Hong, Y. K. Choi, H. Kim and H. H. Yoo, *J. Chromatogr. B*, 2013, **926**, 42–46.
- 55 W.-m. Zhang, W. Qiang, W. Ying-Fei, S. Ming and R. Wang, *J. Pharm. Biomed. Anal.*, 2016, **119**, 45–49.